Antiferromagnetic Dichroism in a Complex Multisublattice Magnetoelectric CuB_2O_4

K. N. Boldyrev,[1,*] R. V. Pisarev,[2] L. N. Bezmaternykh,[3] and M. N. Popova[1]
[1]*Institute of Spectroscopy RAS, 142190 Troitsk, Moscow, Russia*
[2]*Ioffe Physical-Technical Institute RAS, 194021 St. Petersburg, Russia*
[3]*Kirensky Institute of Physics, Siberian Branch RAS, 660036 Krasnoyarsk, Russia*
(Received 30 April 2015; published 19 June 2015)

Magnetic control of the crystal chirality was announced by Saito *et al.* [Phys. Rev. Lett. 101, 117402 (2008)] on the ground of experiments in CuB_2O_4. This claim has raised a sharp dispute in the literature because it seemed to contradict the fundamental symmetry principles. We settle this dispute on the basis of a high-resolution optical spectroscopy study of excitonic transitions in CuB_2O_4. We find that a large sublattice-sensitive antiferromagnetic linear dichroism (LD) emerges at the Néel temperature $T_N = 21$ K and show how it could simulate a "magnetic-field control of the crystal chirality." We prove that the discovered LD is related microscopically to the magnetic Davydov splitting. This LD is highly sensitive to subtle changes in the spin subsystems, which allowed us to observe a splitting of the phase transition into an incommensurate magnetic phase into two transitions ($T_1^* = 8.5$ and $T_2^* = 7.9$ K) and to suggest elliptical spiral structures below T_1^*, instead of a simple circular helix proposed earlier.

DOI: 10.1103/PhysRevLett.114.247210 PACS numbers: 75.25.-j, 75.50.Ee, 75.85.+t, 78.20.Ls

Breaking of time-reversal symmetry at phase transitions or in an external magnetic field leads to fundamental changes in the propagation of light and its interaction with matter [1–7]. For magnetic, magnetoelectric, piezomagnetic, and multiferroic media, time-reversal symmetry breaking, when accompanied by spatial-inversion symmetry breaking, opens new degrees of freedom in the light-matter interaction and results in novel optical phenomena. Those were predicted and then observed in spectral ranges from terahertz to hard x rays. Some examples are the gyrotropic birefringence [8–10], nonreciprocal reflection of light from antiferromagnets [11], magnetochiral and directional dichroism [12–14], quadrochroism [15], etc. Other experimental reports and a detailed symmetry analysis can be found in a review and original papers [4–7,16–18]. Importantly, time-reversal symmetry breaking triggers various nonlinear optical phenomena, e.g., such as spin-sensitive optical harmonics generation [19,20].

A novel effect of this type, namely, magnetic control of crystal chirality was reported on the grounds of experiments with a circularly polarized light resonant with $3d$ excitonic transitions in CuB_2O_4 [21]. However, soon after that the effect was refuted on the basis of a theoretical symmetry analysis [4]. The latter publication was followed by a fierce "comment-reply" discussion raising questions of a fundamental importance whether or not an applied magnetic field can switch the chirality of a crystal [22,23]. At the end of it the participants remained with their own opinions [5,24,25]. We note that the authors of the theoretical works [4,5,23] suggested linear dichroism (LD) as a prime candidate for signals displayed in Ref. [21]; however, up to now LD studies have not been performed for CuB_2O_4. Evidently, the mentioned fundamental controversy can be resolved only by a new task-oriented experimental investigation of magneto-optical properties of CuB_2O_4.

In this Letter, we report results of high-resolution optical spectroscopy studies of CuB_2O_4 with *linearly polarized* light, in the same geometry that was used in the experiments [21] with circularly polarized light. We show that a large sublattice-sensitive linear dichroism emerges below T_N in CuB_2O_4. This observation necessitates a revision of the claims made in Ref. [21]. We elucidate the nature of the discovered antiferromagnetic LD attributing it to the magnetic Davydov splitting. We show that this LD is highly sensitive to subtle changes in the spin subsystems, which allowed us to find a new magnetic phase transition and specify the types of magnetic structures in the incommensurate phases of CuB_2O_4.

Among numerous copper oxides, the metaborate CuB_2O_4 occupies a special position demonstrating a unique combination of magnetic [26–29], magnetoelectric [24,25], and linear and nonlinear optical [30–32] properties. CuB_2O_4 crystallizes in the tetragonal noncentrosymmetric space group $I\bar{4}2d$ (D_{2d}^{12}, $Z = 12$), where the magnetic Cu^{2+} ions ($3d^9$, $S = 1/2$, $L = 0$) occupy two distinct $4b$ and $8d$ square-coordinated positions with the S_4 and C_2 symmetry, respectively [33]. The presence of two different positions for the copper ions leads to a number of interesting and unusual properties. The "strong" magnetic Cu($4b$) subsystem spontaneously orders at the Néel temperature $T_N = 21$ K into an antiferromagnetic commensurate (C) structure with the spins lying in the easy (xy) plane. The Cu($4b$) spins are slightly canted due to the Dzyaloshinskii-Moriya interaction, with a weak ferromagnetic moment along the $\{[110], [\bar{1}\,\bar{1}\,0]\}$ and $\{[1\bar{1}0], [\bar{1}10]\}$ axes allowing two types of 90° antiferromagnetic domains

[26–29]. Elastic [29] and inelastic [34] neutron scattering experiments revealed a quasi-one-dimensionality of the "weak" Cu($8d$) magnetic subsystem. Whereas the Cu($4b$) magnetic moments steadily grow below T_N and reach the value $\mu_{Cu(4b)} = 0.86\mu_B$ (μ_B is the Bohr magneton) at 12 K, the Cu($8d$) ions at the same temperature acquire a small magnetic moment $\mu_{Cu(8d)} = 0.20\mu_B$ along the z axis; it starts to grow only below $T^* = 10$ K, where the phase transition into an incommensurate (IC) helical phase takes place, mounting to the value $\mu_{Cu(8d)} = 0.54\mu_B$ at 2 K [29]. The Cu($8d$) magnetic moments are not completely ordered and fluctuate even at the lowest temperatures.

Plane-parallel polished samples of (010) and (001) orientation and thickness between 50 and 100 μm were prepared from CuB_2O_4 single crystals [35]. Optical transmission spectra were measured with a resolution 0.8 cm^{-1}, using a Bruker IFS 125 HR Fourier spectrometer and a closed-cycle Cryomech ST403 cryostat at the temperatures between 3.2 and 300 K. In addition to conventional absorption measurements in the π ($\mathbf{k}\perp z$, $\mathbf{E}(\omega)\parallel z$), σ ($\mathbf{k}\perp z$, $\mathbf{E}(\omega)\perp z$), and α ($\mathbf{k}\parallel z$, $\mathbf{E}(\omega)$, $\mathbf{H}(\omega)\perp z$) polarizations, we studied the azimuthal angular dependence of the absorption in the (xy) plane, both without and with a magnetic field $\mathbf{B}$ applied along the [110]-or [100]-type directions. It is important to remember that at sufficiently large field ($B \geq B_c = 0.04$ T [27]) antiferromagnetic spins of the Cu($4b$) subsystem are oriented perpendicular to the field $\mathbf{B}$. The LD signal was found as the difference in the absorption coefficient κ for the light polarized along and perpendicular to the direction of antiferromagnetic spins, which are the source of the optical anisotropy below T_N in the (xy) plane.

Figure 1 demonstrates the absorption α spectrum of CuB_2O_4 below T_N. The spectrum in its general features is in agreement with earlier published data [30,31]. Six sharp zero-phonon (ZP) exciton lines originating from the $d-d$ transitions in the Cu^{2+} ions at both the $4b$ and $8d$ positions are followed by broad intense bands with an unusually rich vibronic structure. However, our high-resolution measurements clearly revealed several important details not detected in previous studies. Thus, the second $8d$ and $4b$ lines exhibit a doublet structure due to a low-symmetry component of the crystal field and the spin-orbit interaction, respectively (see the Supplemental Material A [36]). Figures 2(a), 2(b) and 2(c), 2(d) show the temperature behavior of the lowest-frequency $4b$ and $8d$ ZP lines, respectively. Both lines shift and narrow with lowering the temperature, but in a totally different way. Remarkably, all the lines of the strongly coupled Cu($4b$) subsystem quickly broaden and disappear above T_N, whereas the lines of the weak Cu($8d$) subsystem remain observable even above ~100 K. This behavior is very unusual and deserves a more detailed investigation which is out of scope of this Letter. The $4b$ lines demonstrate strikingly pronounced peculiarities at T_N in both the spectral position $\nu(T)$ and the line width $\delta\nu(T)$ dependences. In contrast, the $8d$ lines [Figs. 2(c), 2(d)] remain almost unaltered at T_N but shift and narrow dramatically at the temperature T^* of the second phase transition.

These experimental data point to a distinct coupling of the $3d$ excitons in both copper positions with the relevant

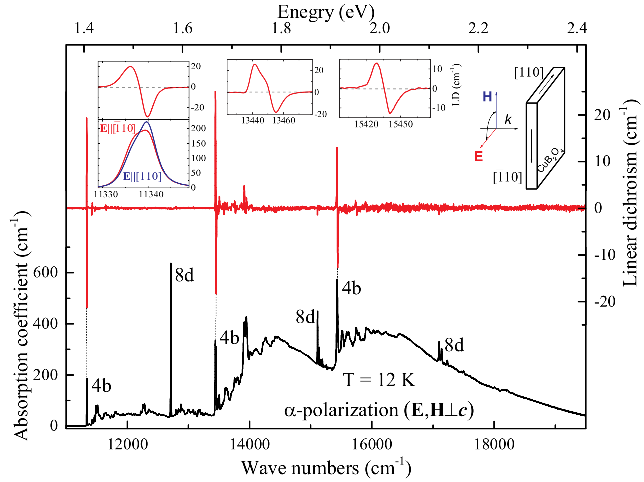

FIG. 1 (color online). Spectra of the α-polarized absorption (lower trace) and the linear dichroism (upper trace) of CuB_2O_4 in the commensurate magnetic phase at $T = 12$ K. ZP lines originating from the $Cu^{2+}(4b)$ and $Cu^{2+}(8d)$ positions are marked in accordance with Ref. [31]. Right inset displays geometry for LD measurements. Lower left inset shows the first $Cu^{2+}(4b)$ ZP line registered in two mutually perpendicular polarizations, $\boldsymbol{E}\parallel[110]$ and $\boldsymbol{E}\parallel[\bar{1}10]$, both for $\boldsymbol{k}\parallel z$, evidencing the Davydov doublet and explaining the observed LD (upper left inset). Pay attention that the $Cu^{2+}(8d)$ ZP lines do not exhibit LD.

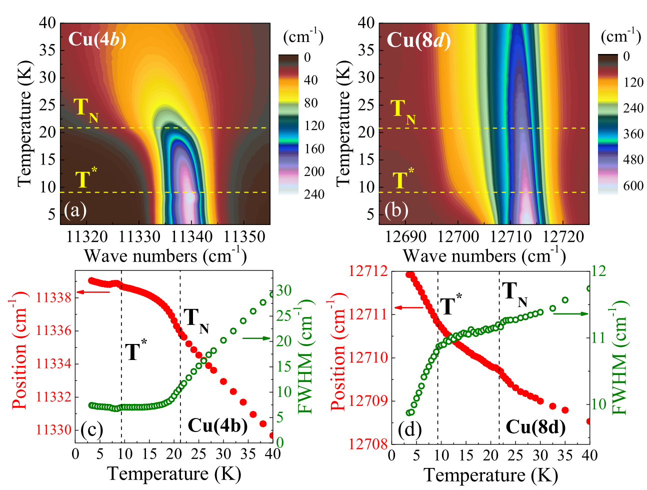

FIG. 2 (color online). Temperature behavior of the lowest-frequency Cu($4b$) and Cu($8d$) ZP α-polarized absorption lines. (a),(b) Color-coded contour plots of the absorption coefficient as a function of temperature vs wave number. The transition temperatures are marked as dotted lines. (c),(d) Temperature dependences of the maximum position and full width at half maximum (FWHM). The error bars are smaller than symbols.

magnetic phase transitions and can be naturally explained in the following way. At T_N, only the Cu$(4b)$ magnetic moments order, which results in shifting the energy levels and freezing the spin fluctuations present in the paramagnetic state. Correspondingly, the $4b$ ZP lines shift and narrow below T_N. A similar scenario takes place at the phase transition at T^* for the Cu$(8d)$ subsystem and the relevant $8d$ spectral lines. Both copper subsystems, Cu$(4b)$ and Cu$(8d)$, are almost independent and therefore the ZP lines of each subsystem demonstrate, predominantly, magnetic properties of the relevant particular subsystem. Nevertheless, weak but well-pronounced features in the $8d$ lines are observed also at T_N, as well as the $4b$ lines show marked frequency changes at T^* (see Fig. 2). This behavior of the $4b$ and $8d$ excitons clearly demonstrates an existence of a coupling between them. Thus, this coupling being too weak to be observable in magnetic measurements [26] finds a clear confirmation in the behavior of the exciton lines.

Next, we discuss important polarization properties of the ZP lines for the case of light propagating along the tetragonal z axis ($\mathbf{k}\|z$). Above T_N, the macroscopic magnetic symmetry of CuB_2O_4 is $\bar{4}2m1'$ and the (xy) plane is magnetically and optically isotropic. Therefore, the absorption for $\mathbf{k}\|z$ is also isotropic and does not depend on the orientation of $\mathbf{E}(\omega)$ with respect to the x or y axes. In other words, linearly and circularly polarized light waves are the degenerate eigenmodes. Though CuB_2O_4 is a noncentrosymmetric crystal, optical activity or chiral dichroism are not allowed. However, right below T_N the antiferromagnetic spins of the Cu$(4b)$ subsystem form two types of domains in the (xy) plane with the spins along the $\{[110],[\bar{1}\,\bar{1}\,0]\}$ and/or $\{[1\bar{1}0],[\bar{1}10]\}$ axes. These domains are characterized by the reduced magnetic point groups $mm'2'$ or $m'm2'$, respectively. The fourfold symmetry axis $\bar{4}$ is reduced to $2'$ and, consequently, the optical isotropy in the (xy) plane is destroyed and the mode degeneracy is lifted. Thus, below T_N the eigenmodes for light propagating along the $2'$ axis are the two linearly polarized orthogonal modes along and perpendicular to the spin orientation. Propagation of circularly polarized modes is forbidden and therefore no chiral dichroism appears below T_N. In contrast, the magnetic point group $mm'2'$ (or $m'm2'$) allows the antiferromagnetic linear dichroism, which is the difference in the absorption of light polarized along and perpendicular to the spin directions [4,5,23,37]. In the case of the $\mathbf{B}\|x([100])$ and $\mathbf{B}\|y([010])$ geometries the magnetic point groups are $22'2'$ and $2'22'$, respectively and, again, the LD is allowed [4,37].

Indeed, an appreciable linear dichroism for all three $4b$ ZP lines is observed below T_N (Fig. 1). As discussed above, one has to keep in mind the existence of two kinds of antiferromagnetic domains giving opposite contributions to the observed effect. Evidently, the magnitude of the LD signal can be considerably enhanced by applying a magnetic field $B \geq B_c = 0.04$ T [27] in the (xy) plane which favors one type of domain at the expense of the other, making a single-domain sample. We have applied a magnetic field of 0.7 T along the [110] direction and observed the fivefold enhancement of LD. We also studied the $\mathbf{B}\|x([100])$ and $\mathbf{B}\|y([010])$ geometries and found that (i) the absolute value of the LD is the same as for the $\mathbf{B}\|[110]$ geometry, and (ii) the LD signal reverses sign under a 90° rotation of the field direction around the z axis. As for the $8d$ ZP lines, none of them show any dichroism in this geometry, which is understandable in view of the alignment of Cu$(8d)$ magnetic moments predominantly along the z axis.

We note that the shape of a dichroic signal (Fig. 1) and its behavior under a 90° rotation of the field direction in our experiments are similar to those observed by Saito *et al.* [21] with the circularly polarized light, whereas its value is about 25 times greater (Fig. 3). We may suggest that the signals in Ref. [21] arose due to a small linearly polarized (LP) component. The ratio $\sim 1/25$ of dichroic signals observed there and in this work, and the absence of a dichroic signal in Ref. [21] for $\mathbf{B}\|[110]$ imply LP components $|S_1| = 0.04$, $|S_2| = 0$ and, hence, a helicity $|S_3| = \sqrt{1 - S_1^2 - S_2^2} = 0.999$. Here, S_i, $i = 1,2,3$, are the Stokes parameters characterizing LP components along the x or y axes (S_1) and at $\pm 45°$ (S_2) and a circularly polarized

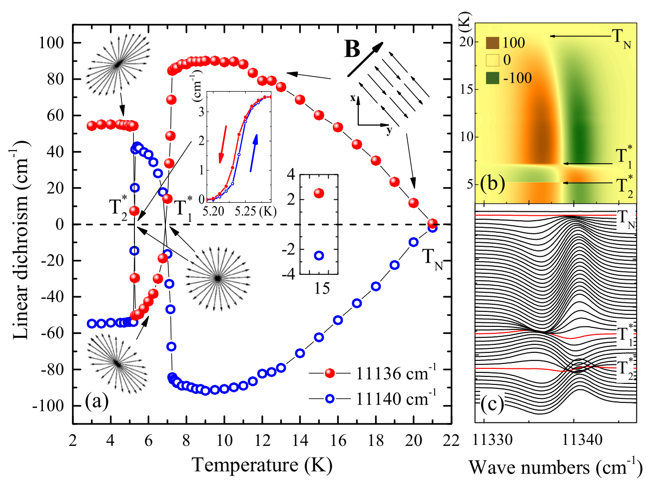

FIG. 3 (color online). (a) Temperature dependence of LD (for the light polarized along and perpendicular to the [110] direction) at 11 136 cm^{-1} (red balls) and 11 140 cm^{-1} (blue circles). $B_{ext} = 0.7$ T is applied along the [110] direction. A splitting of the phase transition at T^* into two transitions (at T_1^* and T_2^*) is evident. Arrows schematically demonstrate proposed magnetic structures. The right Inset shows the "magnetic circular dichroism" data from Ref. [21]. The left Inset displays a hysteresis loop observed in the vicinity of T_2^*. (b),(c) LD spectra in the region of the first $4b$ ZP line of CuB_2O_4 at temperatures below T_N, (for the light polarized along and perpendicular to the [110] direction; $\mathbf{k}\|z$), displayed as (b) color-coded contour plots and (c) shifted plots taken with steps from 0.5 to 0.05 K.

(CP) light (S_3). Suppose the LP component is along the x axis of a $\lambda/4$ plate that produces a circular polarization. To switch from the right-handed to the left-handed CP, the $\lambda/4$ plate has to be rotated by 90° and the LP component also rotates by 90°. Thus, a departure from an ideal circular polarization as small as 0.1% can be responsible for LD signals observed by Saito *et al.* [21], but attributed to magnetic chiral dichroism.

After establishing the presence of a strong antiferromagnetic linear dichroism, the important question arises what is its *microscopic* origin, in particular, for the first ZP line which corresponds to the optical transition $(x^2 - y^2) \rightarrow (xy)$ between two nondegenerate orbital singlets (the Supplemental Fig. S1a [36]). To understand this, we pay attention to the presence of two crystallographically equivalent $\mathrm{Cu}(4b)$ ions in the *primitive* cell of CuB_2O_4. It is known that if there are N equivalent entities in a primitive cell, the corresponding spectral band splits into N bands (the so called Davydov or the factor-group splitting) [38]. In the case the first $4b$ ZP line one might expect a Davydov excitonic doublet which depends on the magnetic structure [38,39]. (In the Supplemental Material B [36], this is explained in detail for the magnetic structure realized in the temperature interval $T^* < T < T_N$). And really, below T_N two orthogonally polarized components, at 11 336 and 11 340 cm^{-1}, are resolved within the first $4b$ ZP line (lower left Inset of Fig. 1).

The strong antiferromagnetic-order-induced linear dichroism discovered in our study opens important opportunities to probe different magnetic phases of a rich $B - T$ phase diagram of CuB_2O_4. Figure 3 shows dichroic signals at the wavelengths of the two Davydov components of the first $4b$ ZP line as functions of temperature, for a single-domain CuB_2O_4 crystal in a magnetic field $\mathbf{B}\|[110]$. Splitting of the $\mathrm{C} \rightarrow \mathrm{IC}$ phase transition at T^* into two transitions ($T_1^* = 7.2$ and $T_2^* = 5.2$ K) is clearly seen, with an intriguing change of the LD sign between T_1^* and T_2^*. Two phase transitions in the vicinity of T^* are clearly observed in our LD spectra also without an external magnetic field. In this case $T_1^* = 8.5$ and $T_2^* = 7.9$ K, i.e., both T_1^* and T_2^* temperatures are higher while the $(T_1^* - T_2^*)$ difference is reduced. This behavior is in agreement with the existence of two different incommensurate magnetic phases in CuB_2O_4 at $T < T^*$ under applied magnetic field $B > 1.2$ T [40]. The nature of these phases was not discussed in Ref. [40] but can be specified from our data in the following way.

Under an external magnetic field, the phase transition at T_1^* is continuous but that at T_2^* is very sharp and demonstrates a small hysteresis (Fig. 3). Among the symmetry allowed magnetic structures in the IC phase of CuB_2O_4, helical structures composed of the basis vectors $\psi_1(\Gamma_i)$ and $\psi_2(\Gamma_i)$, $i = 3$ or 4, of two different Γ_3 or Γ_4 irreducible representations, $c_1\psi_1(\Gamma_i) + c_2\psi_2(\Gamma_i)$, are compatible with neutron scattering data [29]. If $|c_1| = |c_2|$, a simple helical structure is realized, while $|c_1| \neq |c_2|$ leads to an elliptical magnetic structure. These cases could not be distinguished experimentally in Ref. [29]. For the magnetic propagation vector of the IC phase $\boldsymbol{k}_{\mathrm{IC}} \rightarrow 0$, the basis vectors of the Γ_3 representation of the IC phase become identical to those of the C phase and the $\mathrm{C} \rightarrow \mathrm{IC}(\Gamma_3)$ transition is continuous [29]. The $\mathrm{IC}(\Gamma_3) \rightarrow \mathrm{IC}(\Gamma_4)$ transition requires a π phase change in ψ_2 and must be of the first order. These considerations suggest that at T_1^* the $\mathrm{C} \rightarrow \mathrm{IC}(\Gamma_3)$ transition takes place but at T_2^* a transformation $\mathrm{IC}(\Gamma_3) \rightarrow \mathrm{IC}(\Gamma_4)$ occurs.

Our LD data can also elucidate some important features of incommensurate structures in CuB_2O_4. We note that in the case of a simple spin helix suggested in earlier studies [29,41] LD would obviously vanish by symmetry arguments. Experimentally, LD vanishes only at two temperature values, T_1^* and T_2^* (Fig. 3). We may confidently assume that not a simple helix but some kinds of elliptical helical spin structures are realized. A sign change of the LD at T_1^* and once more at T_2^* can be interpreted as a reorientation of the long axis of the spin ellipse at T_1^* and then one more reversal at T_2^*. Detailed measurements of the angular dependences of the dichroic signal at different temperatures show a smooth rotation of the long axis of a spin ellipse below T_1^*. Such a plethora of magnetic structures and phase transitions in CuB_2O_4 evidently takes place due to multiple intricate frustrated and nonfrustrated antisymmetric exchange interactions within and between the magnetic $\mathrm{Cu}(4b)$ and $\mathrm{Cu}(8d)$ subsystems [42].

Thus, the present high-resolution spectroscopic study of exciton lines at both $4b$ and $8d$ magnetic sites in a multisublattice compound CuB_2O_4 evidences a pronounced coupling between optical electronic transitions and transformations in magnetic subsystems. Weak interaction between $\mathrm{Cu}(4b)$ and $\mathrm{Cu}(8d)$ magnetic subsystems is observed, which was not noticed in numerous previous studies by optical and other methods. Our study has allowed us to resolve the magnetic Davydov splitting of the $3d$ copper excitons in a complex magnetoelectric antiferromagnet CuB_2O_4 and, as a consequence, to observe a well-pronounced sublattice-sensitive antiferromagnetic linear dichroism in the crystallographically isotropic (xy) plane of this tetragonal crystal. We have shown that the discovered linear dichroism can serve as a highly sensitive tool for probing magnetic phase transitions and magnetic structures. In particular, we have found a new phase transition between two incommensurate magnetic phases in CuB_2O_4, unnoticed in previous studies, specified the irreducible representations that describe these two IC phases, and suggested an elliptical spin structure that rotates when the temperature is changed. No doubt that such an approach based on general symmetry principles can be applied to the studies of magnetic phase transitions and structures in other materials. Importantly, we have shown that in the presence of a large antiferromagnetic linear dichroism, even a minor deviation from an ideal circular polarization, as small as 0.1%, simulates a circular dichroism compatible with signals reported in Ref. [21]. Thus, our findings agree with the principles of magnetic symmetry and are against the claim that a magnetic field can control the chirality of a crystal.

This study was supported by the Russian Academy of Sciences under the Programs for Basic Research, by the President of the Russian Federation (Grant No. MK-3521.2015.2, K. N. B.), by the Russian Foundation for Basic Research (Grants No. 15-32-20613, K. N. B., and No. 15-02-04222, R. V. P.), and by the Ministry of Education and Science of the Russian Federation (Grant No. 14.B25.0031.25, R. V. P.).

*Corresponding author.
kn.boldyrev@gmail.com

[1] T. H. O'Dell, *Electrodynamics of Magnetoelectric Media* (North-Holland, Amsterdam, 1970).
[2] V. V. Eremenko, N. F. Kharchenko, Yu. G. Litvinenko, and V. M. Naumenko, *Magneto-Optics and Spectroscopy of Antiferromagnets* (Springer-Verlag, New York, 1992).
[3] L. D. Barron, *Molecular Light Scattering and Optical Activity* (Cambridge University Press, Cambridge, England, 2004).
[4] S. W. Lovesey and U. Staub, J. Phys. Condens. Matter **21**, 142201 (2009).
[5] S. W. Lovesey and E. Balcar, Phys. Scr. **81**, 065703 (2010).
[6] D. Szaller, S. Bordács, and I. Kézsmárki, Phys. Rev. B **87**, 014421 (2013).
[7] N. P. Armitage, Phys. Rev. B **90**, 035135 (2014).
[8] R. M. Hornreich and S. Shtrikman, Phys. Rev. **171**, 1065 (1968).
[9] A. A. Mukhin, V. D. Travkin, S. P. Lebedev, A. S Prokhorov, and A. M Balbashov, J. Magn. Magn. Mater. **183**, 157 (1998).
[10] C. M. Varma, Europhys. Lett. **106**, 27001 (2014).
[11] B. B. Krichevtsov, V. V. Pavlov, R. V. Pisarev, and V. N. Gridnev, J. Phys. Condens. Matter **5**, 8233 (1993); Phys. Rev. Lett. **76**, 4628 (1996).
[12] J. Goulon, A. Rogalev, F. Wilhelm, C. Goulon-Ginet, P. Carra, D. Cabaret, and C. Brouder, Phys. Rev. Lett. **88**, 237401 (2002).
[13] M. Kubota, T. Arima, Y. Kaneko, J. He, X. Yu, and Y. Tokura, Phys. Rev. Lett. **92**, 137401 (2004).
[14] I. Kézsmárki, N. Kida, H. Murukava, S. Bordács, Y. Onose, and Y. Tokura, Phys. Rev. Lett. **106**, 057403 (2011).
[15] I. Kézsmárki, D. Szaller, S. Bordács *et al.*, Nat. Commun. **5**, 3203 (2014).
[16] N. F. Kharchenko, Ferroelectrics **162**, 173 (1994).
[17] R. V. Pisarev, Sov. Phys. JETP **31**, 761 (1970); Ferroelectrics **162**, 191 (1994); Ferroelectrics **183**, 39 (1996).
[18] T. Arima, J. Phys. Condens. Matter **20**, 434211 (2008).
[19] M. Fiebig, Th. Lottermoser, D. Fröhlich, A. V. Goltsev, and R. V. Pisarev, Nature (London) **419**, 818 (2002).
[20] M. Fiebig, V. V. Pavlov, and R. V. Pisarev, J. Opt. Soc. Am. B **22**, 96 (2005).
[21] M. Saito, K. Ishikawa, K. Taniguchi, and T. Arima, Phys. Rev. Lett. **101**, 117402 (2008).
[22] T. Arima and M. Saito, J. Phys. Condens. Matter **21**, 498001 (2009).
[23] S. W. Lovesey and U. Staub, J. Phys. Condens. Matter **21**, 498002 (2009).
[24] M. Saito, K. Ishikawa, S. Konno, K. Taniguchi, and T. Arima, Nat. Mater. **8**, 634 (2009).
[25] N. D. Khanh, N. Abe, K. Kubo, M. Akaki, M. Tokunaga, T. Sasaki, and T. Arima, Phys. Rev. B **87**, 184416 (2013).
[26] G. Petrakovskii, D. Velikanov, A. Vorotinov, A. Balaev, K. Sablina, A. Amato, B. Roessli, J. Schefer, and U. Staub, J. Magn. Magn. Mater. **205**, 105 (1999).
[27] M. Boehm, B. Roessli, J. Schefer, B. Ouladdiaf, A. Amato, C. Baines, U. Staub, and G. Petrakovskii, Physica (Amsterdam) **318B**, 277 (2002).
[28] B. Roessli, J. Schefer, G. Petrakovskii, B. Ouladdiaf, M. Boehm, U. Staub, A. Vorotinov, and L. Bezmaternikh, Phys. Rev. Lett. **86**, 1885 (2001).
[29] M. Boehm, B. Roessli, J. Schefer, A. Wills, B. Ouladdiaf, E. Lelievre-Berna, U. Staub, and G. A. Petrakovskii, Phys. Rev. B **68**, 024405 (2003).
[30] R. V. Pisarev, I. Sänger, G. A. Petrakovskii, and M. Fiebig, Phys. Rev. Lett. **93**, 037204 (2004).
[31] R. V. Pisarev, A. M. Kalashnikova, O. Schöps, and L. N. Bezmaternykh, Phys. Rev. B **84**, 075160 (2011).
[32] R. V. Pisarev, K. N. Boldyrev, M. N. Popova, A. N. Smirnov, V. Yu. Davydov, L. N. Bezmaternykh, M. B. Smirnov, and V. Yu. Kazimirov, Phys. Rev. B **88**, 024301 (2013).
[33] M. Martinez-Ripoll, S. Martinez-Carrera, and S. Garcia-Blanco, Acta Crystallogr. Sect. B **27**, 677 (1971).
[34] S. Martynov, G. Petrakovskii, and B. Roessli, J. Magn. Magn. Mater. **269**, 106 (2004).
[35] K. S. Aleksandrov, B. P. Sorokin, D. A. Glushkov, L. N. Bezmaternykh, S. I. Burkov, and S. V. Belushchenko, Phys. Solid State **45**, 41 (2003).
[36] See Supplemental Material at http://link.aps.org/supplemental/10.1103/PhysRevLett.114.247210 for (A) the energy level diagrams of the Cu^{2+} ions in two positions, taking into account the crystal-field and spin-orbit interactions and (B) the magnetic Davydov splitting and selection rules.
[37] R. R. Birss, *Symmetry and Magnetism* (North Holland, Amsterdam, 1967).
[38] A. S. Davydov, *Theory of Molecular Excitons* (Plenum Press, New York, 1971).
[39] R. Loudon, Adv. Phys. **17**, 243 (1968).
[40] Y. Kousaka, S. Yano, M. Nishi, K. Hirota, and J. Akimitsu, J. Phys. Chem. Solids **68**, 2170 (2007).
[41] A. I. Pankrats, G. A. Petrakovskii, M. A. Popov, K. A. Sablina, L. A. Prozorova, S. S. Sosin, G. Szimczak, R. Szimczak, and M. Baran, JETP Lett. **78**, 569 (2003).
[42] S. N. Martynov, JETP Lett. **90**, 55 (2009).